AMERICAN SOCIETY FOR MICROBIOLOGY | Applied and Environmental Microbiology®

BIOTECHNOLOGY

Simultaneous Improvements of *Pseudomonas* Cell Growth and Polyhydroxyalkanoate Production from a Lignin Derivative for Lignin-Consolidated Bioprocessing

Xiaopeng Wang,[a] Lu Lin,[b] Junde Dong,[c,f] Juan Ling,[c,f] Wanpeng Wang,[d] Hongling Wang,[e] Zhichao Zhang,[e] Xinwei Yu[e]

[a]Ocean College, Zhejiang University, Hangzhou, China

[b]Institute of Marine Science and Technology, Shandong University, Shandong, China

[c]CAS Key Laboratory of Tropical Marine Bio-resources and Ecology, Guangdong Provincial Key Laboratory of Applied Marine Biology, South China Sea Institute of Oceanology, Chinese Academy of Sciences, Guangzhou, China

[d]Marine Biogenetic Resources, Third Institute of Oceanography, State Oceanic Administration, Xiamen, China

[e]Zhoushan Municipal Center for Disease Control and Prevention, Zhoushan, Zhejiang, China

[f]Guangdong Provincial Key Laboratory of Applied Marine Biology, South China Sea Institute of Oceanology, Chinese Academy of Sciences, Guangzhou, China

ABSTRACT Cell growth and polyhydroxyalkanoate (PHA) biosynthesis are two key traits in PHA production from lignin or its derivatives. However, the links between them remain poorly understood. Here, the transcription levels of key genes involved in PHA biosynthesis were tracked in *Pseudomonas putida* strain A514 grown on vanillic acid as the sole carbon source under different levels of nutrient availability. First, enoyl-coenzyme A (CoA) hydratase (encoded by *phaJ4*) is stress induced and likely to contribute to PHA synthesis under nitrogen starvation conditions. Second, much higher expression levels of 3-hydroxyacyl-acyl carrier protein (ACP) thioesterase (encoded by *phaG*) and long-chain fatty acid-CoA ligase (encoded by *alkK*) under both high and low nitrogen (N) led to the hypothesis that they likely not only have a role in PHA biosynthesis but are also essential to cell growth. Third, 40 mg/liter PHA was synthesized by strain $A_{phaJ4C1}$ (overexpression of *phaJ4* and *phaC1* in strain A514) under low-N conditions, in contrast to 23 mg/liter PHA synthesized under high-N conditions. Under high-N conditions, strain $A_{alkKphaGC1}$ (overexpression of *phaG*, *alkK*, and *phaC1* in A514) produced 90 mg/liter PHA with a cell dry weight of 667 mg/liter, experimentally validating our hypothesis. Finally, further enhancement in cell growth (714 mg/liter) and PHA titer (246 mg/liter) was achieved in strain $A_{xyl\_alkKphaGC1}$ via transcription level optimization, which was regulated by an inducible strong promoter with its regulator, XylR-P_{xylA}, from the xylose catabolic gene cluster of the A514 genome. This study reveals genetic features of genes involved in PHA synthesis from a lignin derivative and provides a novel strategy for rational engineering of these two traits, laying the foundation for lignin-consolidated bioprocessing.

IMPORTANCE With the recent advances in processing carbohydrates in lignocellulosics for bioproducts, almost all biological conversion platforms result in the formation of a significant amount of lignin by-products, representing the second most abundant feedstock on earth. However, this resource is greatly underutilized due to its heterogeneity and recalcitrant chemical structure. Thus, exploiting lignin valorization routes would achieve the complete utilization of lignocellulosic biomass and improve cost-effectiveness. The culture conditions that encourage cell growth and polyhydroxyalkanoate (PHA) accumulation are different. Such an inconsistency represents a major hurdle in lignin-to-PHA bioconversion. In this study, we traced and compared transcription levels of key genes involved in PHA biosynthesis pathways

Received 15 June 2018 **Accepted** 5 July 2018

Accepted manuscript posted online 20 July 2018

Citation Wang X, Lin L, Dong J, Ling J, Wang W, Wang H, Zhang Z, Yu X. 2018. Simultaneous improvements of *Pseudomonas* cell growth and polyhydroxyalkanoate production from a lignin derivative for lignin-consolidated bioprocessing. Appl Environ Microbiol 84:e01469-18. https://doi.org/10.1128/AEM.01469-18.

Editor Rebecca E. Parales, University of California, Davis

Address correspondence to Lu Lin, linlu623@hotmail.com.

X.W. and L.L. contributed equally to this work.

in *Pseudomonas putida* A514 under different nitrogen concentrations to unveil the unusual features of PHA synthesis. Furthermore, an inducible strong promoter was identified. Thus, the molecular features and new genetic tools reveal a strategy to coenhance PHA production and cell growth from a lignin derivative.

KEYWORDS *Pseudomonas putida*, lignin-consolidated bioprocessing, polyhydroxyalkanoate synthesis

Polyhydroxyalkanoates (PHA) are a class of natural biopolymers that are accumulated by microbes as carbon and energy storage materials (1). They can be used as alternatives to petroleum-based plastics due to their environmentally friendly aspects of sustainability and low CO_2 emissions. In addition, their biocompatibility and biodegradability allow them to be bioimplant materials for medical and therapeutic applications (2). Moreover, their controllable thermal and mechanical properties, as well as diverse molecular weights, allow PHA to function as chemical precursors and methyl ester-based fuels (1, 3, 4). The high PHA content (21% of the cellular dry weight) observed in *Escherichia coli* was biosynthesized from fatty acids as early as 1997 (5). However, due to the high cost of fatty acids and their toxicity to bacteria, researchers have attempted to bioproduce PHA from inexpensive and renewable unrelated carbon sources, e.g., glucose and glycerol (6–8). Lignocellulose is the most abundant resource for sustainable fuels and chemical production. With the development of cellulosic biofuel production, substantial quantities of lignin by-products are expected to be generated, representing the second most abundant feedstock on earth (9). However, the recalcitrant nature of lignins and certain technological barriers limit lignin mainly to production of process heat and power via combustion during cellulosic biofuel production (10–12). Thus, finding an efficient conversion route for lignin to PHA would offer a significant opportunity for the viability and sustainability of modern lignocellulosic biorefineries and offset global energy shortages and climate change (13). A few studies have investigated the feasibility of lignin-to-PHA bioconversion routes, including bacterial screening for lignin-consolidated bioprocessing (14, 15) and integrated biological funneling and chemical catalysis for lignin-to-PHA production (3). However, few studies have attempted to study the PHA biosynthetic pathways when strains are grown using either lignin or its derivatives as a sole carbon source (16), most likely because the complex process of lignin depolymerization in lignin-to-PHA bioconversion has hampered investigations and comparisons between PHA biosynthesis pathways. Thus, the molecular mechanisms of PHA biosynthesis, in which various metabolic pathways of fatty acids interact to mediate carbon flux to PHA biosynthesis pathways under conditions where strains are grown on lignin (or its derivatives), remain elusive.

Pseudomonas species are well-known medium-chain-length PHA (*mcl*-PHA)-producing organisms (17), and recent studies have shown that they are capable of lignin degradation (18). They secrete oxidative enzymes (e.g., laccases and dye peroxidases) to trigger lignin decomposition and generation of lignin oligomers (e.g., β-aryl-ether and coniferyl aldehyde), which are subsequently catabolized via versatile aromatic compound pathways (19–21). In addition, they adapt easily to different environments and have readily available genetic manipulation systems (16, 22). Taken together, these traits indicate they could play a profound role in lignin-to-PHA conversion. *Pseudomonas* species readily accumulate *mcl*-PHA under nutrient imbalances, e.g., nitrogen starvation conditions (1). Under nitrogen limitation, strains usually exhibit poor growth (e.g., lower cell density, lighter cell dry weight, or lower growth rate) (14, 23). It should be noted that cell growth (cell biomass in particular) is a critical factor for total PHA production (7). Such an inconsistency between cell growth and PHA production represents one of three major hurdles in lignin-to-PHA bioconversion, the others being lignin depolymerization and aromatic compound degradation. In fact, numerous studies have investigated the PHA biosynthesis pathways in *Pseudomonas*, where PHA is synthesized via either the β-oxidation pathway or by the *de novo* fatty acid biosynthesis pathway when the organisms are grown on related (e.g., fatty acids) or unrelated (e.g., glucose

and glycerol) carbon sources, respectively (1, 24, 25). Moreover, a large number of strategies have been developed to enhance PHA production, such as reconstructing PHA synthetic pathways in model hosts without the ability for PHA accumulation (e.g., *E. coli*) (6, 7, 25–27). However, simultaneous improvement of both cell growth and PHA production in *Pseudomonas* has not been demonstrated, especially when lignin or its derivatives are used as sole carbon sources. Devising a rational strategy to counter this hurdle may require a mechanistic understanding of the links between the two traits.

Here, we employed the previously identified lignin-utilizing *Pseudomonas putida* strain A514 as a research model to investigate the PHA biosynthesis pathways. To simplify the lignin depolymerization process, we utilized a lignin substitute, vanillic acid, a key intermediate metabolite that connects several peripheral pathways to the central pathway (β-ketoadipate pathway) during lignin depolymerization, as the sole carbon source (Fig. 1A) (16, 18). The transcription levels of key genes involved in PHA biosynthesis were tracked and compared when A514 cells were grown on M9 medium with low (65 mg/liter) and high (1 g/liter) nitrogen (N) concentrations, unveiling unusual features of PHA synthesis. Exploiting these molecular features and developing genetic tools enabled us to devise a rational strategy to coenhance PHA production and cell growth.

RESULTS

Transcriptional comparison revealed specific features of PHA synthesis in A514 when a lignin derivative was used as the sole carbon source. *P. putida* A514 was grown on either high-N or low-N M9 medium, supplemented with 15 mM vanillic acid as the sole carbon source. First, it was observed that the doubling time of A514 cells grown on high-N medium (4.8 h) was higher than that of cells grown on low-N medium (3.8 h) during the exponential phase (Table 1 and Fig. S1 in the supplemental material). Second, cell dry weight (CDW) under high-N conditions was approximately 6-fold higher than under low-N conditions (Table 1). Third, 15 mM vanillic acid was completely consumed under high-N growth conditions, whereas only 6.5 mM vanillic acid was utilized under low-N conditions (Table 1 and Fig. S1). Taken together, these results indicate a likely change in gene expression in A514 between the high-N and low-N growth conditions. Thus, the transcription levels of genes involved in PHA synthesis under these two conditions were subsequently examined by reverse transcription-quantitative PCR (qRT-PCR) (Table 2).

Similarly to that of *P. putida* strain KT2440, the A514 *pha* gene cluster consists of *phaC1* and *phaC2*, encoding two polymerases, *phaZ*, encoding a depolymerase, *phaD*, encoding a transcriptional regulator, and two genes encoding polyhydroxyalkanoate granule-associated proteins (*phaF* and *phaI*) (see Fig. S2 in the supplemental material). The organization of these genes in the A514 genome is also similar to that of *P. putida* KT2440, consistent with previous studies showing that the PHA biosynthetic gene cluster is well conserved among the *Pseudomonas* PHA producer strains (17) (Fig. S2). Comparison of gene transcription under high-N and low-N conditions revealed several characteristics of PHA synthesis in A514 when employing a lignin derivative (vanillic acid) as the sole carbon source. First, genes located in the PHA synthesis cluster were upregulated, including *phaC1* (PputA514_5834), *phaC2* (PputA514_5836), *phaD* (PputA514_5837), *phaF* (PputA514_5838), and *phaI* (PputA514_5839) (Fig. 1D and G), confirming the phenotype that PHA synthesis was induced under nitrogen deprivation (Fig. S1). Second, *phaG* (PputA514_1318) and *alkK* (PputA514_1839) were induced (Fig. 1B and E). *phaG* (encoding 3-hydroxyacyl-ACP thioesterase), combined with *alkK* (encoding fatty acid-CoA ligase), provides 3-hydroxyacyl-CoA, the precursor for PHA synthesis (6), thus connecting the *de novo* fatty acid biosynthesis pathway and the PHA biosynthesis pathway. The induced *phaG* gene demonstrated its role in PHA synthesis in the presence of vanillic acid as the carbon source. In addition, nine paralogs that are homologous to the *alkK* gene from *P. putida* KT2440 were identified in A514, and their transcription levels were examined (6, 28). Among them, PputA514_1839 (encoding a long-chain fatty acid-CoA ligase) was prominent in that it not only encoded the highest

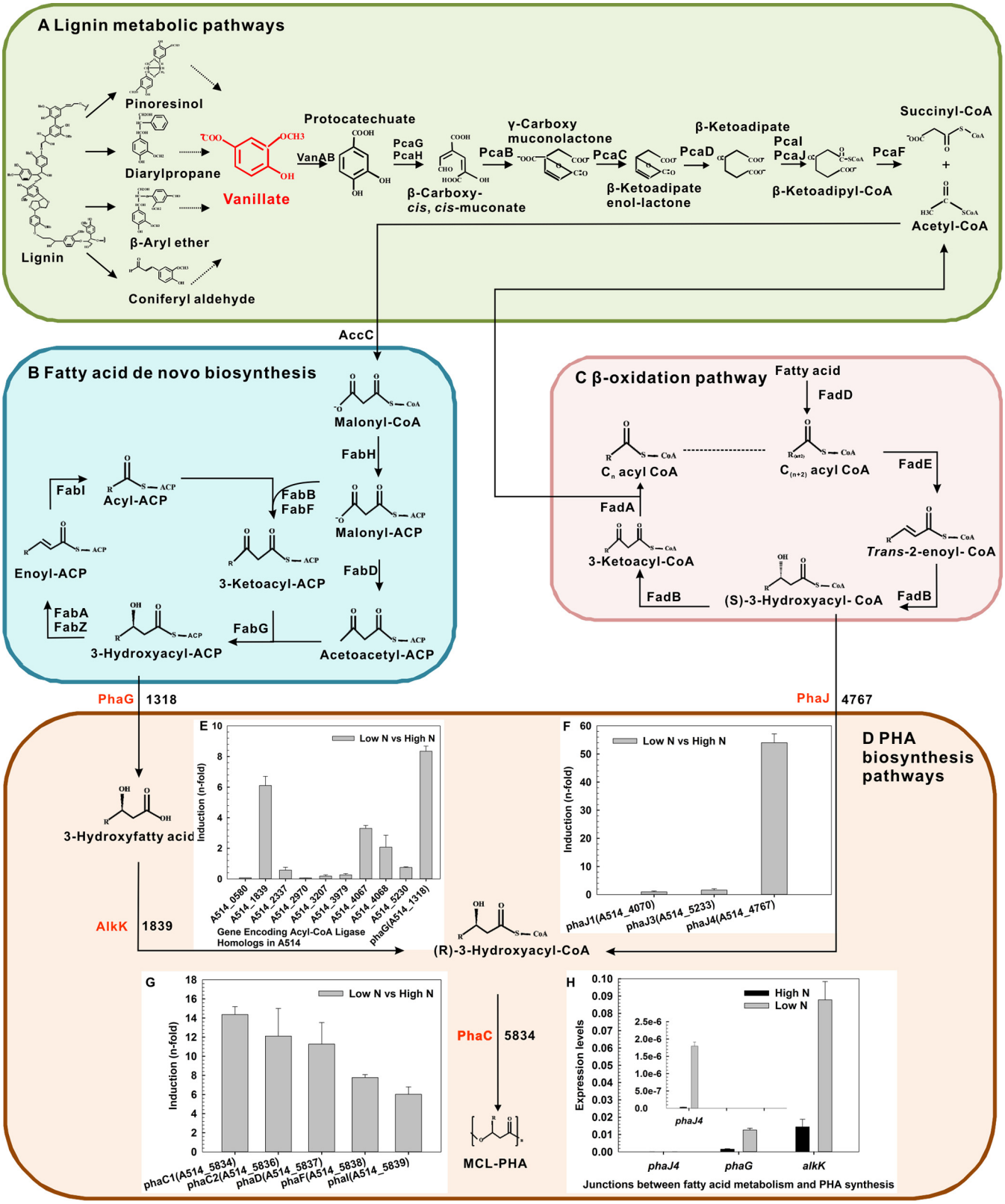

FIG 1 Proposed metabolic pathways for lignin-to-PHA bioconversion. Key genes and metabolic intermediates are highlighted in red. Identifications (IDs) of the corresponding genes in A514 are shown. (A) Lignin degradation pathways. Dashed arrows indicate multiple steps. (B) *De novo* fatty acid biosynthesis. (C) *β*-Oxidation pathway. After each turn of the cycle, an acyl-CoA (indicated as C_n) that is two carbons shorter than the initial one (indicated as C_{n+2}) is generated. The dashed line connects acyl-CoA intermediates of different chain lengths. (D) PHA biosynthesis pathways. (E, F, and G) Expression ratios for *alkK* homologs and *phaG* and *phaJ* genes, as well as for PHA synthetic genes, in A514 that were grown under the low-N conditions, compared to those grown under the high-N

(Continued on next page)

TABLE 1 Cell growth and *mcl*-PHA accumulation in the recombinant *P. putida* A514 strains

Culture[a]	Strain	Relevant plasmid	Doubling time[b] (h)	VA[c] utilization (mM)	CDW[d] (mg/liter)	PHA titer (mg/liter)	PHA content (wt %)
High N (1 g/liter)	A514 WT	None	4.8 ± 0.2	14.9 ± 0.01	664.1 ± 3.6	11 ± 2.0	1.7 ± 0.3
	A_{Pvan}	pPvan	4.7 ± 0.3	14.8 ± 0.01	664.6 ± 2.2	12 ± 1.2	1.8 ± 0.2
	$A_{phaJ4C1}$	pTJ4C1	4.6 ± 0.3	15.0 ± 0.02	668.0 ± 3.5	23 ± 1.0	3.4 ± 0.2
	$A_{alkKphaGC1}$	pTphaGC1	4.5 ± 0.2	14.9 ± 0.01	667.5 ± 4.8	90 ± 2.1	13.5 ± 0.3
	$A_{R\text{-}PxylA}$	$pTRP_{xylA}$	4.9 ± 0.4	15.0 ± 0.01	694.7 ± 11.1	12 ± 0.6	1.7 ± 0.2
	$A_{xyl\_phaJ4C1}$	pTP_{xylA}phaGC1	4.8 ± 0.1	15.0 ± 0.02	702.7 ± 19.4	26 ± 1.7	3.7 ± 0.3
	$A_{xyl\_alkKphaGC1}$	$pTP_{xylA}phaJ4C1$	4.8 ± 0.2	15.0 ± 0.01	714.8 ± 12.9	246 ± 17.3	34.4 ± 0.3
Low N (65 mg/liter)	A514 WT	None	3.8 ± 0.3	6.5 ± 0.03	133.8 ± 10.9	23 ± 1.0	17.3 ± 1.8
	A_{Pvan}	pPvan	3.7 ± 0.2	6.6 ± 0.06	135.5 ± 5.8	23 ± 3.8	17.1 ± 2.1
	$A_{phaJ4C1}$	pTJ4C1	3.7 ± 0.2	7.4 ± 0.05	133.0 ± 7.8	43 ± 1.5	32.6 ± 1.2
	$A_{alkKphaGC1}$	pTphaGC1	3.9 ± 0.1	7.6 ± 0.05	145.2 ± 7.3	62 ± 6.1	42.4 ± 2.2
	A_{R_PxylA}	$pTRP_{xylA}$	3.8 ± 0.2	7.5 ± 0.04	148.7 ± 6.1	24 ± 0.6	16.6 ± 1.1
	$A_{xyl\_phaJ4C1}$	pTP_{xylA}phaGC1	3.7 ± 0.3	7.9 ± 0.04	141.3 ± 12.3	63 ± 2.3	44.5 ± 4.9
	$A_{xyl\_alkKphaGC1}$	$pTP_{xylA}phaJ4C1$	3.5 ± 0.1	8.7 ± 0.04	175.3 ± 13.3	116 ± 4.5	66.3 ± 4.7

[a]The strains were grown in 15 mM vanillic acid-M9 medium under either high-N (1 g/liter) or low-N (65 mg/liter) conditions.
[b]The doubling time (DT) was calculated during the exponential phase, based on the formula $DT = t \cdot [\log 2/(\log N_t - \log N_0)]$.
[c]VA, vanillic acid.
[d]CDW, cell dry weight.

protein identity (89%; E value, 0) to AlkK of *P. putida* KT2440, but also showed the highest level of transcription (Fig. 1E), suggesting its probable contribution in the production of 3-hydroxyacyl-CoA for PHA production. Third, *phaJ4*, which connects the β-oxidation pathway and the PHA synthesis pathway, was highly upregulated (~54-fold) (Fig. 1C and F). *phaJ* [encoding (*R*)-specific enoyl-CoA hydratase] produces 3-hydroxyacyl-CoA from fatty acid oxidation as the precursor for PHA biosynthesis (7). A514 harbors three *phaJ* paralogs, namely, *phaJ1* (PputA514_4070), *phaJ3* (PputA514_5233), and *phaJ4* (PputA514_4767). Among them, *phaJ4* exhibited the highest induction (Fig. 1F), suggesting an important role for this gene in directing carbon flux from the β-oxidation pathway to PHA biosynthesis. This is consistent with our previous study, where overexpressing *phaJ4* and *phaC1* increased PHA production when lignin was used as the sole carbon source (16). Fourth, compared to *phaJ4*, *phaG* and *alkK* sustained much higher expression levels under both high- and low-N conditions, indicating that, in addition to PHA synthesis, they were likely to be important in cell growth (Fig. 1H). Furthermore, comparison of low-N and high-N conditions showed that *phaJ4* was highly induced (~54-fold), in contrast to *phaG* and *alkK*, which showed only ~6-fold activation (Fig. 1E and F). This was distinct from the PHA-producing model strain, *P. putida* KT2440, where it was *phaG* that presented the greatest induction (~220-fold versus 3.8-fold for *phaJ4*) when grown on low-N medium compared to high-N medium (6), suggesting specific features of PHA synthesis in A514 when utilizing vanillic acid as the carbon source.

Increasing carbon flux from *de novo* fatty acid biosynthesis to PHA synthesis can simultaneously improve PHA production and cell growth. Our previous study demonstrated that *phaJ4* and *phaC1* are important for PHA biosynthesis from lignin under nitrogen starvation conditions in A514 cultures (16). However, the unique transcriptional feature of *phaG* and *alkK*, in this study, suggested their role in both PHA biosynthesis and cell survival, thus raising the feasibility of enhancing PHA production without impairing cell growth. To validate this hypothesis, the plasmid pPvan, plasmid pPROBE-TT carrying the P_{van} promoter, was employed as the expression vector (Table 3) (29). *phaG* (PputA514_1318), *alkK* (PputA514_1839), and *phaC1* (PputA514_5834) were cloned into pPvan to construct the plasmid pTphaGC1, while *phaJ4* (PputA514_4767) and

FIG 1 Legend (Continued)
conditions. The ratios that were >1 were defined as induced. (H) Expression levels of the *phaJ4*, *phaG*, and *alkK* (PputA514_1839) genes in A514 under both high-N and low-N conditions. The inset in panel H shows the expression level of *phaJ4* at an appropriate scale. The expression levels and expression ratios are defined in Materials and Methods.

TABLE 2 Primers used in qRT-PCR

Primer	Sequences
PputA514_5834	F: 5′-TCACCGCCGACATCTACTC-3′; R: 5′-CTGCTGGACAACACGAACTC-3′
PputA514_5836	F: 5′-CACTTCGCATTCGCCTTGT-3′; R: 5′-TGTTGCCGCCTGAGTTGA-3′
PputA514_5834	F: 5′-GCGACCGTATCCTTGAATGT-3′; R: 5′-GAAGTGGTAGTAGAGGTTGCC-3′
PputA514_5838	F: 5′-GCGTCTCAACAGTGCTAT-3′; R: 5′-TTTGCTTGGTCAGGGTATC-3′
PputA514_5839	F: 5′-AGTAATGTCTCAAGCGTCAA-3′; R: 5′-TGCCGATTCGATTCAAGG-3′
PputA514_4767	F: 5′-ATTATGTCGGCAAGGAACT-3′; R: 5′-GACGTGGATGAACTGATGA-3′
PputA514_4070	F: 5′-TGTTCAAGGAGCGTATCG-3′; R: 5′-GGCTTCTGGAAGGTCATC-3′
PputA514_5233	F: 5′-CAAAGGTCTTTGGCTTTCGC-3′; R: 5′-CAGGAAGATTGGCAGCTTGA-3′
PputA514_1318	F: 5′-GCCTGTATCCGCAATTCAAC-3′; R: 5′-CCTTCGTCAGCATCTTCTCAT-3′
PputA514_1839	F: 5′-CCAGATCGCCGTTGTTACT-3′; R: 5′-GCCTGCCATTCAATGATGTC-3′
PputA514_2970	F: 5′-TCAGGATCAGGACCTTGC-3′; R: 5′-GCGTAACACAGCGACATA-3′
PputA514_4067	F: 5′-CCACATCTATGCCTTCACCTT-3′; R: 5′-CTTCCACTTCGACAGTTCCTT-3′
PputA514_4068	F: 5′-GGTTCGTGAGCATTGTTG-3′; R: 5′-CGTCTTCGATCTCGTTGG-3′
PputA514_5230	F: 5′-CAAAGACCCGAACCTGACTC-3′; R: 5′-TGCTGCGAAACTCCACATAC-3′
PputA514_3207	F: 5′-ACCACAACATCCTCAACAA-3′; R: 5′-ATACCGAAGCAGTGATACAA-3′
PputA514_0580	F: 5′-TGTGGAACTGGCTGGTGTC-3′; R: 5′-GCTGATTGTCTCGGCATCG-3′
PputA514_3979	F: 5′-TGAAGATGGCTACTGGTGGAT-3′; R: 5′-TCGGCGACTTTAGGGTGAG-3′
PputA514_2337	F: 5′-CCATCCGATCACCTTCTACGA-3′; R: 5′-GGCAATCAGCAGGCGATAC-3′
PputA514_4978	F: 5′-GGCAACGAAGTGGATGAA-3′; R: 5′-CTGGCAACGGATGATGTC-3′

phaC1 (PputA514_5834) were cloned into pPvan, generating the pTJ4C1 vector. The three plasmids were subsequently transformed into strain A514, generating the recombinant strains A_{Pvan}, $A_{alkKphaGC1}$, and $A_{phaJ4C1}$, respectively (Table 3). $A_{alkKphaGC1}$ was subsequently characterized for cell growth and PHA production, while $A_{phaJ4C1}$ and A_{Pvan} were used as reference strains.

Under nitrogen excess conditions, $A_{alkKphaGC1}$ showed significant improvement in PHA titer, which increased to 90 mg/liter, although levels of cell growth and vanillic acid utilization for all three strains were similar (Table 1 and Fig. S3A). Under nitrogen limitation conditions, $A_{alkKphaGC1}$ showed improvement in cell biomass compared to that of A_{Pvan} ($P = 0.016$; Table 1 and Fig. S3B). In addition, $A_{alkKphaGC1}$ produced 54% and 166% more PHA than did $A_{phaJ4C1}$ and A_{Pvan}, respectively, reaching ~62 mg/liter (Table 1 and Fig. S3B). Corresponding to the higher CDW and PHA titer, more vanillic acid was consumed by $A_{alkKphaGC1}$ than by A_{Pvan} ($P = 0.006$, Table 1 and Fig. S3B).

These data demonstrate two aspects of the mechanism for PHA biosynthesis from vanillic acid. First, although increasing 3-hydroxyacyl-CoA from either the *de novo* fatty acid biosynthesis pathway or β-oxidation pathway improved PHA production, overex-

TABLE 3 Plasmids and bacterial strains used in this study

Strain or plasmid	Relevant characteristic(s)	Source and/or reference
Plasmids		
pPROBE-TT		30
pPvan	pPROBE-TT derivative, *P. putida* A514 promoter of *vanAB* (P_{van})	This study
pTJ4C1	pPROBE-TT derivative, P_{van}, *phaJ4*, and *phaC1*	This study
pTphaGC1	pPROBE-TT derivative, P_{van}, *phaG*, *alkK*, and *phaC1*	This study
pTP_{xylA}	pPROBE-TT derivative, *P. putida* A514 promoter of *xylA* (P_{xylA})	This study
$pTRP_{xylA}$	pPROBE-TT derivative, P_{xylA}, and *xylR*	This study
pTP_{xylA}phaGC1	pPROBE-TT derivative, P_{xylA}, *phaG*, *alkK*, and *phaC1*	This study
pTP_{xylA}phaJ4C1	pPROBE-TT derivative, P_{xylA}, *phaJ4*, and *phaC1*	This study
Strains		
P. putida A514	Wild type	Dennis Gross lab (TAMU) (17)
A_T	A514 carrying pPROBE-TT	This study
A_{Pvan}	A514 carrying pPvan	This study
$A_{phaJ4C1}$	A514 carrying pTJ4C1	This study
$A_{alkKphaGC1}$	A514 carrying pTphaGC1	This study
A_{PxylA}	A514 carrying pTP_{xylA}	This study
$A_{R\text{-}PxylA}$	A514 carrying $pTRP_{xylA}$	This study
$A_{xyl\_phaJ4C1}$	A514 carrying pTP_{xylA}phaJ4C1	This study
$A_{xyl\_alkKphaGC1}$	A514 carrying pTP_{xylA}phaGC1	This study

pression of *phaG* and *alkK* contributed more to PHA production in strain A514, especially under conditions of excess nitrogen (Table 1 and Fig. S3). Second, when A514 cells were grown under conditions favoring PHA accumulation (nutrition imbalance), enhancing the expression levels of *phaG* and *alkK* coimproved cell growth and PHA biosynthesis. On the basis of these results, we experimentally validated the role of *phaG* and *alkK* in PHA production and cell growth, and we suggest that this property could be further exploited to coenhance cell growth and PHA production.

Screening an inducible strong promoter to regulate the transcription levels of *phaG* and *alkK* from strain A514. In $A_{alkKphaGC1}$, the PHA synthetic gene cluster from pTphaGC1 was constitutively expressed in the presence of vanillic acid, as the promoter P_{van} was induced by vanillic acid (Table 3). PHA synthesis, thereby, was turned on during the initial cell growth period, likely causing a burden on $A_{alkKphaGC1}$. Consequently, to further increase PHA production, an alternative inducible strong promoter was required to regulate the relevant gene expression.

For this purpose, a putative xylose catabolism gene cluster (*xylAFGH*), which appeared to be specifically induced by xylose, was targeted based on our previous genomics data (Fig. 2A) (16). The promoter sequence (P_{xylA}) is located in the 160-bp intergenic region shared by the *xylR* (xylose operon regulatory protein) and *xylA* (xylose isomerase) genes. It was predicted by the PePPER webserver and cloned into the promoter probe vector pPROBE-TT, with a *gfp* (green fluorescent protein gene) reporter gene, generating the pTP_{xylA} construction (29, 30) (Table 3). When A_{PxylA} (carrying pTP_{xylA} in A514) was grown in M9 medium supplemented with 15 mM vanillic acid (rather than with xylose), the measured green fluorescence was close to background levels observed in A514 cells harboring the plasmid pPROBE-TT (designated A_T) (Fig. 2B, bars 1 and 2, and Table 3). In contrast, an obvious green fluorescent signal was detected with the addition of xylose, confirming that the activity of P_{xylA} was specifically induced by xylose (Fig. 2B, bar 3).

To maximize the activity of P_{xylA}, three crucial factors were investigated, as follows: the regulator, induced expression time, and inducer concentrations. First, *xylR* (PputA514_3011) enhanced the activity of P_{xylA}. *xylR* is located immediately upstream of the *xylAFGH* cluster, with its transcription oriented in the opposite direction, suggesting a role in modulating *xylAFGH* expression in response to xylose (Fig. 2A). Therefore, we created a recombinant strain, $A_{R\text{-}PxylA}$, bearing $pTRP_{xylA}$ (Table 3). When assayed in $A_{R\text{-}PxylA}$, the promoter activity was distinctly enhanced, 2.4-fold higher than that with P_{xylA} (Fig. 2B, bars 3 and 5), confirming that XylR is a positive regulator for P_{xylA}. Second, a higher promoter activity was found when xylose was added during the mid-exponential phase. To examine the effect of the induced expression time on the P_{xylA} activity, 0.2 mM xylose (final concentration) was added at three time points (during the early-to-mid exponential phase), and the level of green fluorescence was measured from time of addition to stationary phase. When xylose was added during the early exponential phase (optical density at 600 nm [OD_{600}], ~0.36), promoter activity in A_{PxylA} was quickly switched on, reaching highest activity at 3 h and sustained at this level until stationary phase (15 h after induction began). In contrast, when xylose was added during the mid-exponential phase (OD_{600}, ~0.56 and ~0.78), promoter activity increased along with the induced expression time and reached the highest activity at 12 h (stationary phase). Since higher green fluorescence intensity was detected in A_{PxylA} when xylose was supplemented at the mid-exponential phase than at the early exponential phase, xylose was added at the mid-exponential phase (e.g., at OD_{600} of ~0.78) for the following study (Fig. 2C). Third, there was an inducer concentration-dependent effect on promoter activity, with a final concentration of 2 mM xylose being determined as the appropriate concentration. To assess the effect of different xylose concentrations, $A_{R\text{-}PxylA}$ was grown in M9 medium with 15 mM vanillic acid, reaching an OD_{600} of ~0.78, and then exposed to various inducer concentrations (from 0.02 mM to 20 mM) for 6 h (Fig. 2D). It was determined that 2 mM xylose was sufficient to activate P_{PxylA}.

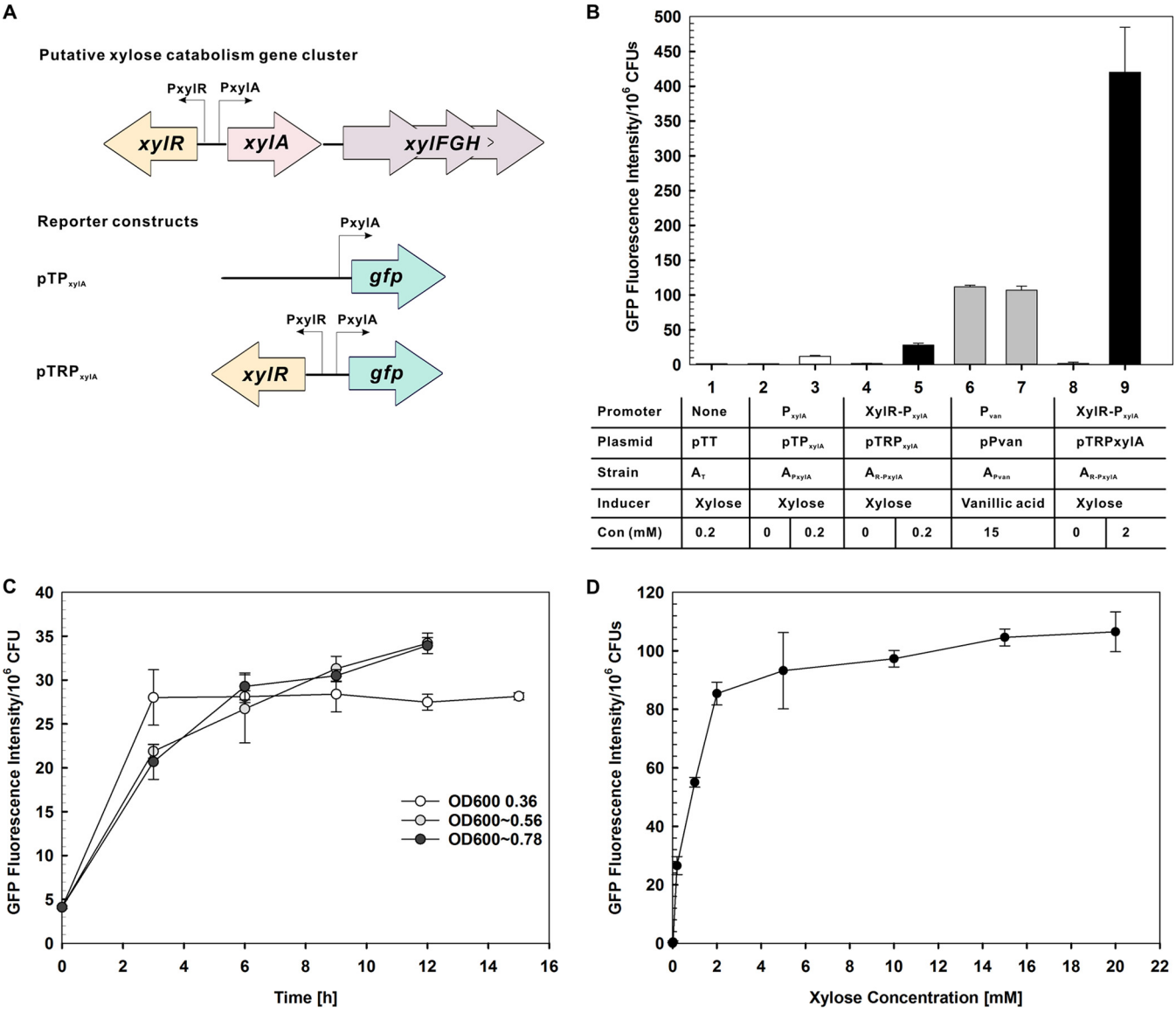

FIG 2 Effect of the regulator, regulator-induced expression time, and inducer concentrations on the activity of the promoter P_{xylA}. (A) Organization of the putative A514 xylose catabolism locus, as well as reporter constructs used to detect activity of P_{xylA}. P, promoter; *gfp*, green fluorescent protein gene. (B) Activities of P_{xylA} and P_{van} under various inducing conditions. For bars 1 to 5, either 0 mM or 0.2 mM (final concentration) xylose was added when strains were at the mid-exponential phase. After 6 h of induction, green fluorescence intensity was measured to determine the promoter activity. Bars 6 and 7 represent the P_{van} activity in A_{Pvan} at the mid-exponential phase and the stationary phase, respectively. Bars 8 and 9 represent the XylR-P_{xylA} activity in $A_{R\text{-}PxylA}$ at the stationary phase, which was exposed to 0 mM or 2 mM xylose for 12 h, respectively. pTT, pPROBE-TT; Con, concentration. (C) Time point-dependent induction of XylR-P_{xylA} activity. Response of XylR-P_{xylA} to different growth phases at which 0.2 mM xylose (final concentration) was added. Fluorescence intensity was measured every 3 h until $A_{R\text{-}PxylA}$ entered the stationary phase. (D) Xylose concentration-dependent induction of XylR-P_{xylA} activity. $A_{R\text{-}PxylA}$ at the mid-exponential phase was exposed to different concentrations of xylose for 6 h. For panels B, C, and D, all of the strains were cultivated in M9 medium supplemented with 15 mM vanillic acid. Fluorescence intensity, which was detected to determine the promoter activity, is expressed in arbitrary units normalized for 10^6 CFU.

Therefore, the optimized promoter activity of XylR-P_{xylA} in the expression vector pTRP$_{xylA}$ was achieved when adding 2 mM xylose at an OD_{600} of ~0.78 and was approximately 4-fold higher than that of A_{Pvan} under 15 mM vanillic acid conditions (Fig. 2B, bars 7 and 9).

PHA production was further enhanced via transcription level optimization. Next, the expression vector pTRP$_{xylA}$ was employed to coexpress the two PHA synthetic gene clusters in A514. Thus, two recombinant strains, $A_{xyl\_phaJ4C1}$ and $A_{xyl\_alkKphaGC1}$, were generated. Substrate utilization, cell growth, and PHA titers of these two strains were assessed (Table 1 and Fig. S4). (i) More vanillic acid was utilized by $A_{xyl\_alkKphaGC1}$

TABLE 4 GC compositional analysis of *mcl*-PHA produced by recombinant *P. putida* A514 strains[a]

Strain	Culture	PHA composition (mol%)[b]				
		3HHx (C_6)	3HO (C_8)	3HD (C_{10})	3HDD (C_{12})	3HTD (C_{14})
A_{Pvan}	High N (1 g/liter)	56.0 ± 4.8	ND	21.7 ± 1.2	22.3 ± 1.0	ND
$A_{phaJ4C1}$		53.6 ± 2.1	ND	25.7 ± 1.5	20.7 ± 1.7	ND
$A_{alkKphaGC1}$		15.0 ± 1.0	20.0 ± 1.9	47.8 ± 3.1	14.9 ± 2.2	2.3 ± 0.6
$A_{R\text{-}PxylA}$		57.4 ± 5.0	ND	19.9 ± 0.6	22.7 ± 1.0	ND
$A_{xyl\_phaJ4C1}$		56.8 ± 1.0	ND	20.6 ± 0.8	22.6 ± 1.1	ND
$A_{xyl\_alkKphaGC1}$		10.2 ± 0.8	30.9 ± 1.8	41.2 ± 1.5	15.2 ± 0.7	2.5 ± 0.1
A_{Pvan}	Low N (65 mg/liter)	44.2 ± 0.3	8.3 ± 1.0	20.2 ± 1.2	13.4 ± 2.0	13.9 ± 0.6
$A_{phaJ4C1}$		33.2 ± 0.5	11.9 ± 0.8	25.8 ± 2.3	12.1 ± 1.5	17.0 ± 1.0
$A_{alkKphaGC1}$		17.0 ± 1.1	18.3 ± 1.0	34.1 ± 2.1	12.1 ± 2.9	18.5 ± 0.3
$A_{R\text{-}PxylA}$		45.4 ± 2.8	7.3 ± 0.2	16.6 ± 2.0	14.9 ± 0.7	15.8 ± 0.4
$A_{xyl\_phaJ4C1}$		32.5 ± 0.9	9.8 ± 0.9	24.7 ± 2.3	13.8 ± 1.2	19.2 ± 0.1
$A_{xyl\_alkKphaGC1}$		16.0 ± 0.8	15.2 ± 2.6	32.8 ± 1.7	13.1 ± 0.4	22.9 ± 0.1

[a]Vanillic acid (15 mM) was used as the carbon source.
[b]3HHx, 3-hydroxyhexanoate; 3HO, 3-hydroxyoctanoate; 3HD, 3-hydroxydecanoate; 3HDD, 3-hydroxydodecanoate; 3HTD, 3-hydroxytetradecanoate; ND, not detected.

than by $A_{alkKphaGC1}$ under nitrogen deprivation conditions ($P = 6 \times 10^{-6}$, Table 1 and Fig. S3 and S4). A similar trend was observed in $A_{xyl\_phaJ4C1}$, in contrast to in $A_{phaJ4C1}$ ($P = 1 \times 10^{-4}$). (ii) In comparison with $A_{alkKphaGC1}$, cell growth was further improved in $A_{xyl\_alkKphaGC1}$, especially under nitrogen starvation conditions. The growth rate and cell biomass of $A_{xyl\_alkKphaGC1}$ were both enhanced under the low-N conditions ($P = 0.008$ for doubling time and $P = 0.019$ for CDW; Table 1). In addition, a higher cell biomass of $A_{xyl\_alkKphaGC1}$ was also obtained under the high-N conditions ($P = 0.003$; Table 1). (iii) $A_{xyl\_alkKphaGC1}$ and $A_{xyl\_phaJ4C1}$ produced more PHA titer than $A_{alkKphaGC1}$ and $A_{phaJ4C1}$, respectively (P values < 0.05), whereas A_{Pvan} and $A_{R\text{-}PxylA}$ produced PHA titers similar to that of A514 (P values > 0.05; Table 1 and Fig. S3 and S4). This indicated that the PHA titer was improved by regulating the transcription levels of key genes. A514 and A_{Pvan} cultures (carrying promoter P_{van} in the plasmid pPROBE-TT) were grown in vanillic acid-M9 medium, while $A_{R\text{-}PxylA}$ cells (carrying promoter R-P_{xylA} in the plasmid pPROBE-TT) were grown in vanillic acid-M9 medium with 2 mM xylose inducer added at the mid-exponential phase (OD_{600}, ~0.78). The similar PHA titers among the three strains (P values > 0.05) suggested that 2 mM xylose has very little contribution to PHA synthesis. (iv) Although the highest PHA content (wt %, 66) was reached in $A_{xyl\_alkKphaGC1}$ under low-N conditions, the greatest PHA titer was produced by $A_{xyl\_alkKphaGC1}$ under high-N conditions, reaching ~250 mg/liter in a single fermentation batch (Table 1 and Fig. S4B). This would be the result of more cell biomass being obtained in $A_{xyl\_alkKphaGC1}$ under high-N conditions, demonstrating the role of the cell biomass in PHA production. (v) Gas chromatography-mass spectrometry (GC-MS) composition analysis revealed that the PHA produced were medium-chain-length PHA (*mcl*-PHA) (C_6 to C_{14}). Compared to that in $A_{R\text{-}PxylA}$, the major units in $A_{xyl\_alkKphaGC1}$ PHA polymers were shifted from shorter-carbon-chain units to longer-carbon-chain units. Under nitrogen starvation conditions, 3-hydroxydecanoate (3HD, C_{10}) (~33%) and 3-hydroxytetradecanoate (3HTD, C_{14}) (~23%) were the major units in $A_{xyl\_alkKphaGC1}$, while the 3HD and 3HTD content in *mcl*-PHA synthesized in $A_{xyl\_phaJ4C1}$ also increased. In contrast, the major PHA component of $A_{R\text{-}PxylA}$ was 3-hydroxyhexanoate (3HHx, C_6), ~45% (Table 4). Under nitrogen excess conditions, 3HD (~41%) and 3-hydroxyoctanoate (3HO, C_8) (~31%) were the major monomers in $A_{xyl\_alkKphaGC1}$, while 3HHx accounted for approximately ~57% of the PHA polymers of $A_{R\text{-}PxylA}$. In particular, 3HTD (~3%) was detected in *mcl*-PHA produced by $A_{xyl\_alkKphaGC1}$, whereas it was not found in *mcl*-PHA produced by $A_{R\text{-}PxylA}$ or $A_{xyl\_phaJ4C1}$ (Table 4).

DISCUSSION

PHA are polyesters that are synthesized by microbes as storage materials and are substantially accumulated under conditions where fatty acids are employed as the feedstock, without the requirement of inorganic ion deprivation. However, the high cost of fatty acids hinders commercialization of PHA production. Therefore, lignin, a

by-product generated in large volumes by lignocellulosic biorefineries, is the ideal substrate for PHA production. When lignin is utilized as a carbon source, PHA accumulation usually occurs under conditions of fluctuating nutrient availability due to its function as a carbon and energy storage molecule. However, this nutrition imbalance generally limits cell growth, which is a critical factor for the total PHA titer and thus represents one of the major hurdles in a consolidated lignin-to-PHA bioconversion scheme. Previous studies have reported strategies for heterologous PHA production without compromising cell biomass in *E. coli*, with either glucose or glycerol as the sole carbon source (6, 7, 31–33), but not, as yet, with lignin or its derivatives. This is probably due to *E. coli*'s inability to degrade lignin, restricting it to glycerol or other carbohydrates. Therefore, testing and comparing the PHA synthetic pathways when lignin or its derivatives are provided as the main source of carbon may serve as an essential foundation for engineering these two traits in *Pseudomonas* species, organisms known to be capable of both lignin degradation and PHA accumulation.

First, our work extended molecular tools for *Pseudomonas* strains by identifying a xylose-inducible promoter, P_{xylA}, which is specifically induced by xylose at a concentration (2 mM) that is sufficient to stimulate its activity without interfering with cell growth when a lignin derivative is utilized as the sole carbon source. Moreover, the adjacent xylose operon regulatory protein, XylR, was validated to stimulate its activity. Thus, XylR-P_{xylA} might be superior for the control of strongly transcribed genes, complementary to an inducible weak promoter, P_{van} (16, 34).

Second, our study unveiled unique features of the *P. putida* A514 *mcl*-PHA biosynthetic genes when this strain is grown on a lignin derivative. Comparison of low-N versus high-N conditions revealed that *phaJ4* exhibited the highest induction (Fig. 1F). This contradicts the current notion that *phaG*, but not *phaJ4*, is significantly upregulated when *P. putida* KT2440 is grown with glycerol (6). The stress-induced *phaJ4* gene should play an important role in PHA biosynthesis under low-N conditions, which is consistent with the result where $A_{xyl\_phaJ4C1}$ generated more *mcl*-PHA under low-N conditions than did A_{R_PxylA} (Table 1). In addition, comparison of the expression levels of *phaG* and *alkK* to *phaJ4* leads to the hypothesis that *phaG* and *alkK* not only have a role in PHA biosynthesis but are also likely to be essential in cell growth (Fig. 2). This hypothesis was validated by the experiment where $A_{xyl\_alkKphaGC1}$ coenhanced the PHA titer and cell growth under both low-N and high-N conditions (Table 1). Furthermore, total PHA titer reached the highest level (~250 mg/liter) under high-N conditions, although the PHA content in $A_{xyl\_alkKphaGC1}$ was not the highest (~35 wt% CDW), possibly a consequence of $A_{xyl\_alkKphaGC1}$ having the highest cell dry weight.

Third, the *mcl*-PHA, synthesized in $A_{xyl\_phaJ4C1}$ and $A_{xyl\_alkphaGC1}$, have a greater number of longer-chain monomers (Table 4). This phenotype may be ascribed to the functions of *phaJ4*, *phaG*, and *alkK*. $phaJ4_{Pa}$ in *P. aeruginosa* encodes an (*R*)-specific enoyl-CoA hydratase that shows specificity for the hydration of longer-chain-length enoyl-CoAs (C_6 to C_{12}) (35). The higher contents of 3HO, 3HDD, and 3HTD in $A_{xyl\_phaJ4C1}$ cells under nitrogen deprivation indicated the homologous *phaJ4* gene in A514 likely has greater preference for C_8, C_{10}, and C_{14} substrates. In addition, the function of PhaG (in *P. putida* KT2440) has been shown as a 3-hydroxyacyl-ACP thioesterase to produce 3-hydroxy fatty acids, while AlkK (in *Pseudomonas oleovorans*) is involved in catalyzing the conversion of 3-hydroxy fatty acids to the PHA precursor 3-hydroxyacyl-CoA (6, 28). The closest homolog in A514 to the AlkK gene is the gene encoding a long-chain fatty acid-CoA ligase (PputA514_1839). Thus, the longer chain PHA monomers (C_{10} and C_{14}) produced in $A_{xyl\_alkphaGC1}$ appear to be the result of *alkK* substrate specificity in A514. This is consistent with the previous report that the *mcl*-PHA synthesized in recombinant *E. coli*, carrying the vector to coexpress PhaG, PhaC1, and the medium-chain fatty acid-CoA ligase (AlkK-like protein in KT2440), mainly contain C_8 and C_{10} (6).

Finally, compared to other studies on PHA biosynthesis from lignin or its derivatives, higher PHA production (246 mg/liter) and cell dry weights (715 mg/liter) were generated in batch cultivation (Table 5). Although a slightly higher PHA titer (252 mg/liter) was produced by *P. putida* KT2440 from alkaline pretreated liquor, it was obtained

TABLE 5 Comparison of the *mcl*-PHA or *scl*-PHA (PHB) production from lignin or its derivatives

Strain	Carbon substrate	Cultivation mode	Cultivation time (h)	CDW (mg/liter)	*mcl*-PHA[a] titer (mg/liter)	*scl*-PHA[b] titer (mg/liter)	PHA content (wt%)	Source or reference
Cupriavidus basilensis B-8	5 g/liter soluble lignin	Shake flask batch	120	736	ND[c]	128	17	38
Pandoraea sp. ISTKB	2 g/liter vanillic acid	Shake flask batch	96	215	ND	72	33	37
P. putida JCM13063	10 g/liter vanillic acid	Shake flask batch	72	210	ND	tr[d]	<1	10
P. putida Gpo1	10 g/liter vanillic acid	Shake flask batch	72	140	ND	tr	<1	10
P. putida KT2440	2 g/liter coumaric acid	Shake flask batch	48	470	160	ND	34	3
P. putida KT2440	2 g/liter ferulic acid	Shake flask batch	48	436	170	ND	39	3
P. putida $A_{xyl\_alkKphaGC1}$	2.5 g/liter vanillic acid	Shake flask batch	50	715	246	ND	34	This study
P. putida KT2440	90% alkaline-pretreated liquor	Fed-batch fermentation	48	787	252	ND	32	3

[a]*mcl*-PHA, medium-chain-length PHA.
[b]*scl*-PHA, short-chain-length PHA.
[c]ND, not determined.
[d]tr, trace.

through fed-batch fermentation and high substrate concentrations (including those of glucose, acetate, coumaric acid, and ferulic acid) (3). Additionally, the monomeric composition and content of PHA produced by bacterial strains from lignin or its derivatives are very important, as they can greatly affect the properties of PHA copolymers (36). Both *Cupriavidus basilensis* B-8 and *Pandoraea* sp. strain ISTKB produce short-chain-length PHA (*scl*-PHA, C_3 to C_5), whereas the monomeric content of *mcl*-PHA generated by *P. putida* KT2440 from alkaline pretreated liquor was not reported (Table 5) (10, 37, 38). In contrast, longer-chain monomers produced by A514 in general and the large amount of longer monomers (e.g., 3HTD) synthesized by $A_{xyl\_alkphaGC1}$ in particular would have higher crystallinity and better tensile strength (36), which may endow *mcl*-PHA with novel mechanical properties and wider array of potential applications. This demonstrated that increasing the expression levels of *phaG* and *alkK* is a more efficient strategy to coenhance PHA titer and cell growth, and that *P. putida* $A_{xyl\_alkKphaGC1}$ is a very competitive strain for the production of PHA from lignin derivatives.

Conclusions. In summary, this study revealed specific features of the PHA synthesis pathways for *P. putida* A514 when grown using a lignin derivative and demonstrated a rational strategy to coengineer cell growth and PHA production. As improvements in cell growth and bioproduct production are crucial and shared goals in the sustainable development of lignocellulosic biorefineries (11), our findings should be valuable not just to the production of PHA, but also to that of a wide variety of biofuels and biochemicals. Further genetic strategies, including optimization of the carbon flux either from *de novo* fatty acid biosynthesis or β-oxidation pathways to PHA synthesis (e.g., deletion, insertion, or substitution of the genes involved in fatty acid metabolism, global nitrogen regulation, and so on), and fermentation optimization at flask level or bioreactor level in the near future would further improve the PHA content in cells, which then could be integrated into lignin-consolidated bioprocessing to promote the production of bioproducts.

MATERIALS AND METHODS

Bacterial strains and growth conditions. The strains and plasmids used in this study are summarized in Table 3. *E. coli* DH5α was used for all molecular manipulations to construct plasmids. This strain was grown on Luria-Bertani (LB) medium at 37°C. During recombinant plasmid construction, 15 μg/ml tetracycline was added to the medium. For *P. putida* A514 and cultivation of its recombinant strains, all strains were grown on LB agar for 24 h at 30°C. A single colony was inoculated into 5 ml of 15 mM vanillic acid-M9 mineral medium (with a high concentration NH_4Cl [1 g/liter]) and grown at 30°C with shaking at 200 rpm (39). When the stationary phase was reached, 0.2 ml of culture solution was transferred into 20 ml of fresh vanillic acid-M9 mineral medium with either high-concentration NH_4Cl (1 g/liter) or low-concentration NH_4Cl (65 mg/liter) at 30°C, 200 rpm, and passaged two times (with 1% [vol/vol] inoculation) under the same culture condition. Subsequently, 1% (vol/vol) of seed inoculum for shake flask cultivation was incubated in 100 ml of vanillic acid-M9 mineral medium with high-N or low-N conditions at 30°C and 200 rpm. Tetracycline (15 μg/ml) was added to the medium when culturing *P. putida* A514 recombinant strains. Cell growth was spectrophotometrically monitored by measuring the optical densities at 600 nm (OD_{600}). For the cultivation of strains $A_{R\text{-}PxylA}$, $A_{xyl\_phaJ4C1}$, and $A_{xyl\_alkKphaGC1}$, xylose was introduced to a final concentration of 2 mM when the OD_{600} was either ~0.78 (in the high-nitrogen culture medium) or ~0.22 (in the low-nitrogen culture medium). The doubling times (DT) of all the strains were calculated during the exponential phase, based on the formula $DT = t \cdot [\log 2/(\log N_t - \log N_0)]$, where t = duration, N_t = final cell concentration, and N_0 = initial cell concentration. To determine the number of living cells of N_0 and N_t, 100 μl of fermentation culture was serially diluted and plated on LB agar plates. CFU/ml was assessed as cell concentration. All of the experiments were performed in biological triplicate and technical duplicate.

Determination of gene transcription levels by qRT-PCR. qRT-PCR was performed as previously described (40). Briefly, a total volume of 10 ml of *P. putida* A514 cell culture was harvested from either high-nitrogen (OD_{600}, ~0.78) or low-nitrogen (OD_{600}, ~0.22) culture medium during the mid-exponential phase. The total RNA was isolated using a TransZol Up Plus RNA kit (Transgen Biotech). cDNA libraries were synthesized with a TransScript one-step genomic DNA (gDNA) removal and cDNA synthesis supermix kit (Transgen Biotech), employing 0.5 μg of total RNA as the template for each sample. The qRT-PCRs were performed using the SYBR Premix *Ex Taq* II kit (TaKaRa) with the real-time PCR detection system (Applied Biosystems VII A7). The primers used in qRT-PCR are listed in Table 2. Gene expression levels were assessed by comparing the ratios of the housekeeping gene *rpoD* (PputA514_4978, encoding the housekeeping σ^{70} factor) threshold cycle (C_T) values to target gene C_T values using the following equation: ratio of *rpoD*/target $= 2^{CT(rpoD) - CT(target)}$ (6). The *n*-fold induction was determined by the expression levels of the genes of cells grown on low-N M9 medium versus those of cells grown on high-N M9 medium. All of the samples were prepared and analyzed in biological triplicate and technical duplicate.

Plasmid and strain construction. A 315-bp PCR fragment containing the promoter fragment of the *vanAB* genes (encoding vanillate demethylase A and vanillate *O*-demethylase oxidoreductase in the vanillic acid degradation pathway), P_{van}, was amplified from *P. putida* A514 genomic DNA and subsequently ligated into the plasmid pPROBE-TT (29) through HindIII and EcoRI, to generate the plasmid pPvan. pPvan was used as the expression vector for coexpression of PHA synthesis genes. The putative 3-hydroxyacyl-ACP thioesterase gene (*phaG*, PputA514_1318), long-chain fatty acid-CoA ligase gene (*alkK*, PputA514_1839), enoyl-CoA hydratase gene (*phaJ4*, PputA514_4767), and poly(3-hydroxyalkanoate) polymerase 1 gene (*phaC1*, PputA514_5834) were amplified by PCR from the genome of A514. These three DNA fragments (*phaG*, *alkK*, and P_{van}) were fused by gene splicing by overlap extension (SOE) PCR to produce a 2.8-kb PCR fragment, whereas the DNA fragments of *phaJ4* and P_{van} were fused to produce a 0.78-kb PCR fragment. The two overlap PCR fragments were digested with HindIII and KpnI, respectively, while the *phaC1* fragment was digested with KpnI and EcoRI. DNA fragments containing P_{van}, *phaG*, *alkK*, and *phaC1* were cloned into the pPROBE-TT to construct plasmid pTphaGC1. Similarly, DNA fragments containing P_{van}, *phaJ4*, and *phaC1* were cloned into the pPROBE-TT to construct the pTJ4C1 vector (Table 3).

For the inducible promoter investigation, a chromosomal fragment comprising the 140-bp *xylR-xylA* intergenic region was PCR amplified and cloned into the plasmid pPROBE-TT through HindIII and XbaI, generating the pTP_{xylA} vector (29). To construct $pTRP_{xylA}$, a genomic fragment containing the ORF region of *xylR* and the *xylR-xylA* intergenic region was PCR amplified, digested by HindIII and XbaI, and then ligated into the pPROBE-TT (Table 3).

The plasmid $pTRP_{xylA}$ was used as the expression vector to coexpress the PHA synthesis genes. A DNA fragment containing *phaC1* and either *phaG* and *alkK* or *phaJ4* was amplified and cloned into $pTRP_{xylA}$ to construct pTP_{xylA}phaGC1 and pTP_{xylA}phaJ4C1, respectively (Table 3).

All plasmids were verified by DNA sequencing and were subsequently transformed into A514 cells through chemical transformation (41), followed by selection on LB agar supplemented with 15 μg/ml tetracycline.

Green fluorescence signal detection. Cells from 15 mM vanillic acid-M9 medium cultures were harvested, centrifuged, washed once with 10 mM phosphate buffer, and then resuspended in phosphate buffer. Fluorescence was measured on an LS50B luminescence spectrometer (PerkinElmer Instruments, Norwalk, CT) at an excitation wavelength of 490 nm, an emission wavelength of 510 nm, and emission/excitation slit widths of 8 nm. Intensity readings are represented by arbitrary units and were normalized to a cell density of 10^6 CFU/ml. All of the experiments were performed in biological triplicate and technical duplicate.

Analytical procedures. To measure the concentration of vanillic acid in the medium, 1-ml cell samples were centrifuged for 5 min at 16,000 $\times$ *g*, and the concentration of vanillic acid in the supernatant was measured via absorbance at 289 nm, as previously described (16). For PHA production analysis, PHA biosynthesis and monomer compositions were analyzed by gas chromatography-tandem mass spectrometry (GC-MS/MS; Agilent, Santa Clara, CA). PHA titer was defined as the PHA concentration (mg) per one liter of shake flask batch culture, while PHA content was defined as the percentage of PHA concentration (mg) to cell dry weight (mg). Liquid cultures (100 ml) were harvested at the stationary phase and centrifuged at 9,000 $\times$ *g* for 15 min at 4°C, washed twice with 15 ml Nanopure water, lyophilized (Lyophilizer Alpha 1-4 LSC; Martin Christ Gefriertrocknungsanlagen GmbH, Osterode am Harz, Germany) at −59°C and 0.140 $\times$ 10^5 mPa for a minimum of 24 h, and weighed. The lyophilized cells were dissolved in 2 ml of methanol-sulfuric acid (85:15) solution and 2 ml chloroform (containing a final concentration of 0.01 mg/ml 3-methylbenzoic acid as the internal standard) and then incubated at 100°C for 4 h to methanolysis. After cooling, 1 ml of demineralized water was added to the organic phase, which contained the resulting methyl esters of monomers. The organic phase was filtered and analyzed by GC-MS/MS (Agilent series 7890B GC system; Santa Clara, CA), coupled with a 7000D MS detector (extractor ion [EI]; 70 eV). An aliquot (1 μl) of the organic phase, which was properly diluted, was injected into the gas chromatography column. Separation of compounds was achieved using an HP-5 capillary column (5% phenyl-95% methyl siloxane, 30 m by 0.32-mm inside diameter [i.d.] by 0.25-μm film thickness). Helium was used as the carrier gas at a flow rate of 1.1 ml/min. The injector and transfer line temperatures were set at 280°C and 300°C, respectively. The oven temperature program was as follows: initial temperature of 60°C for 3 min, then from 60°C to 200°C at a rate of 5°C per min, then 200°C for 1 min, and finally from 200°C to 280°C a rate of 15°C per min. The EI mass spectrum was recorded in full scan mode (*m/z* 40 to 550). PHA standard samples (3HHx, 3HO, 3HD, 3HDD, and 3HTD), which were purchased from Sigma-Aldrich, Larodan, and TRC, were also analyzed by GC-MS/MS according to the method above. The retention time (RT), patterns of fragment ion peaks for known PHA standards, and resulting mass spectra available compared with the GC-MS library database (NIST08s) were all employed to determine the PHA monomers in the study samples (7, 23). All of the experiments were performed in biological triplicate and technical duplicate. Differences between groups (including cell dry weight, vanillic acid concentration, and PHA titer) were evaluated using two-tailed unpaired *t* tests. Those with *P* values of <0.05 are considered significant.

SUPPLEMENTAL MATERIAL

Supplemental material for this article may be found at https://doi.org/10.1128/AEM.01469-18.

SUPPLEMENTAL FILE 1, PDF file, 0.7 MB.

ACKNOWLEDGMENTS

This work was supported by grant 41606154 from the NSF of China; grant LMB17011002 from the Open Funding of Key Laboratory of Tropical Marine Bioresources and Ecology, Chinese Academy of Sciences; grant HY201704 from the Open Funding of Key Laboratory of Marine Biogenetic Resources, Third Institute of Oceanography, State Oceanic Administration; and grant SKYAM002-2016 from the State Key Laboratory of Applied Microbiology Southern China, Guangdong Institute of Microbiology. The funders had no role in the study design, data collection and analysis, decision to publish, or preparation of the manuscript.

L.L. conceived and designed the experiments. L.L. and X.W. performed the experiments. L.L. analyzed the data and wrote the paper. J.D., J.L., W.W., H.W., Z.Z., and X.Y. contributed reagents, materials, and analysis tools. All authors read and approved the final manuscript.

We declare that we have no conflicts of interest.

REFERENCES

1. Wang Y, Yin J, Chen GQ. 2014. Polyhydroxyalkanoates, challenges and opportunities. Curr Opin Biotechnol 30:59–65. https://doi.org/10.1016/j.copbio.2014.06.001.
2. Zhang J, Shishatskaya EI, Volova TG, da Silva LF, Chen GQ. 2018. Polyhydroxyalkanoates (PHA) for therapeutic applications. Mater Sci Eng C Mater Biol Appl 86:144–150. https://doi.org/10.1016/j.msec.2017.12.035.
3. Linger JG, Vardon DR, Guarnieri MT, Karp EM, Hunsinger GB, Franden MA, Johnson CW, Chupka G, Strathmann TJ, Pienkos PT, Beckham GT. 2014. Lignin valorization through integrated biological funneling and chemical catalysis. Proc Natl Acad Sci U S A 111:12013–12018. https://doi.org/10.1073/pnas.1410657111.
4. Chen GQ, Hajnal I, Wu H, Lv L, Ye J. 2015. Engineering biosynthesis mechanisms for diversifying polyhydroxyalkanoates. Trends Biotechnol 33:565–574. https://doi.org/10.1016/j.tibtech.2015.07.007.
5. Langenbach S, Rehm BH, Steinbuchel A. 1997. Functional expression of the PHA synthase gene phaC1 from *Pseudomonas aeruginosa* in *Escherichia coli* results in poly(3-hydroxyalkanoate) synthesis. FEMS Microbiol Lett 150:303–309. https://doi.org/10.1111/j.1574-6968.1997.tb10385.x.
6. Wang Q, Tappel RC, Zhu C, Nomura CT. 2012. Development of a new strategy for production of medium-chain-length polyhydroxyalkanoates by recombinant *Escherichia coli* via inexpensive non-fatty acid feedstocks. Appl Environ Microbiol 78:519–527. https://doi.org/10.1128/AEM.07020-11.
7. Zhuang QQ, Wang Q, Liang QF, Qi QS. 2014. Synthesis of polyhydroxyalkanoates from glucose that contain medium-chain-length monomers via the reversed fatty acid beta-oxidation cycle in *Escherichia coli*. Metab Eng 24:78–86. https://doi.org/10.1016/j.ymben.2014.05.004.
8. Burniol-Figols A, Varrone C, Le SB, Daugaard AE, Skiadas IV, Gavala HN. 2018. Combined polyhydroxyalkanoates (PHA) and 1,3-propanediol production from crude glycerol: selective conversion of volatile fatty acids into PHA by mixed microbial consortia. Water Res 136:180–191. https://doi.org/10.1016/j.watres.2018.02.029.
9. Lin L, Xu J. 2013. Dissecting and engineering metabolic and regulatory networks of thermophilic bacteria for biofuel production. Biotechnol Adv 31:827–837. https://doi.org/10.1016/j.biotechadv.2013.03.003.
10. Tomizawa S, Chuah J-A, Matsumoto K, Doi Y, Numata K. 2014. Understanding the limitations in the biosynthesis of polyhydroxyalkanoate (PHA) from lignin derivatives. ACS Sustainable Chem Eng 2:1106–1113. https://doi.org/10.1021/sc500066f.
11. Ragauskas AJ, Beckham GT, Biddy MJ, Chandra R, Chen F, Davis MF, Davison BH, Dixon RA, Gilna P, Keller M, Langan P, Naskar AK, Saddler JN, Tschaplinski TJ, Tuskan GA, Wyman CE. 2014. Lignin valorization: improving lignin processing in the biorefinery. Science 344:1246843. https://doi.org/10.1126/science.1246843.
12. Wyman CE. 2007. What is (and is not) vital to advancing cellulosic ethanol. Trends Biotechnol 25:153–157. https://doi.org/10.1016/j.tibtech.2007.02.009.
13. Gao X, Chen J-C, Wu Q, Chen G-Q. 2011. Polyhydroxyalkanoates as a source of chemicals, polymers, and biofuels. Curr Opin Biotechnol 22:768–774. https://doi.org/10.1016/j.copbio.2011.06.005.
14. Salvachua D, Karp EM, Nimlos CT, Vardon DR, Beckham GT. 2015. Towards lignin consolidated bioprocessing: simultaneous lignin depolymerization and product generation by bacteria. Green Chem 17:4951–4967. https://doi.org/10.1039/C5GC01165E.
15. Numata K, Morisaki K. 2015. Screening of marine bacteria to synthesize polyhydroxyalkanoate from lignin: contribution of lignin derivatives to biosynthesis by *Oceanimonas doudoroffii*. ACS Sustainable Chem Eng 3:569–573. https://doi.org/10.1021/acssuschemeng.5b00031.
16. Lin L, Cheng Y, Pu Y, Sun S, Li X, Jin M, Pierson EA, Gross DC, Dale BE, Dai SY, Ragauskas AJ, Yuan JS. 2016. Systems biology-guided biodesign of consolidated lignin conversion. Green Chem 18:5536–5547. https://doi.org/10.1039/C6GC01131D.
17. Prieto MA, Eugenio LId, Galàn B, Luengo JM, Witholt B. 2007. Synthesis and degradation of polyhydroxyalkanoates, p 397–428. *In* Ramos J-L, Filloux A (ed), *Pseudomonas*: a model system in biology. Springer Netherlands, Dordrecht, the Netherlands.
18. Bugg TD, Ahmad M, Hardiman EM, Singh R. 2011. The emerging role for bacteria in lignin degradation and bio-product formation. Curr Opin Biotechnol 22:394–400. https://doi.org/10.1016/j.copbio.2010.10.009.
19. Rahmanpour R, Bugg TD. 2015. Characterisation of Dyp-type peroxidases from *Pseudomonas fluorescens* Pf-5: oxidation of Mn(II) and polymeric lignin by Dyp1B. Archives of biochemistry and biophysics 574:93–98. https://doi.org/10.1016/j.abb.2014.12.022.
20. de Gonzalo G, Colpa DI, Habib MH, Fraaije MW. 2016. Bacterial enzymes involved in lignin degradation. J Biotechnol 236:110–119. https://doi.org/10.1016/j.jbiotec.2016.08.011.
21. Santos A, Mendes S, Brissos V, Martins LO. 2014. New dye-decolorizing peroxidases from *Bacillus subtilis* and *Pseudomonas putida* MET94: towards biotechnological applications. Appl Microbiol Biotechnol 98:2053–2065. https://doi.org/10.1007/s00253-013-5041-4.
22. Nikel PI, Martinez-Garcia E, de Lorenzo V. 2014. Biotechnological domestication of *Pseudomonads* using synthetic biology. Nat Rev Microbiol 12:368–379. https://doi.org/10.1038/nrmicro3253.
23. Nikodinovic-Runic J, Flanagan M, Hume AR, Cagney G, O'Connor KE. 2009. Analysis of the *Pseudomonas putida* CA-3 proteome during growth on styrene under nitrogen-limiting and non-limiting conditions. Microbiology 155:3348–3361. https://doi.org/10.1099/mic.0.031153-0.
24. Moita R, Freches A, Lemos PC. 2014. Crude glycerol as feedstock for polyhydroxyalkanoates production by mixed microbial cultures. Water Res 58:9–20. https://doi.org/10.1016/j.watres.2014.03.066.
25. Wang Q, Nomura CT. 2010. Monitoring differences in gene expression levels and polyhydroxyalkanoate (PHA) production in *Pseudomonas putida* KT2440 grown on different carbon sources. J Biosci Bioeng 110:653–659. https://doi.org/10.1016/j.jbiosc.2010.08.001.
26. Poblete-Castro I, Escapa IF, Jager C, Puchalka J, Lam CM, Schomburg D, Prieto MA, Martins dos Santos VA. 2012. The metabolic response of *P. putida* KT2442 producing high levels of polyhydroxyalkanoate under single- and multiple-nutrient-limited growth: highlights from a multi-level omics approach. Microb Cell Fact 11:34. https://doi.org/10.1186/1475-2859-11-34.
27. Ryan WJ, O'Leary ND, O'Mahony M, Dobson AD. 2013. GacS-dependent regulation of polyhydroxyalkanoate synthesis in *Pseudomonas putida*

CA-3. Appl Environ Microbiol 79:1795–1802. https://doi.org/10.1128/AEM.02962-12.
28. Satoh Y, Murakami F, Tajima K, Munekata M. 2005. Enzymatic synthesis of poly(3-hydroxybutyrate-co-4-hydroxybutyrate) with CoA recycling using polyhydroxyalkanoate synthase and acyl-CoA synthetase. J Biosci Bioeng 99:508–511. https://doi.org/10.1263/jbb.99.508.
29. Miller WG, Leveau JH, Lindow SE. 2000. Improved *gfp* and *inaZ* broad-host-range promoter-probe vectors. Mol Plant Microbe Interact 13:1243–1250. https://doi.org/10.1094/MPMI.2000.13.11.1243.
30. de Jong A, Pietersma H, Cordes M, Kuipers OP, Kok J. 2012. PePPER: a webserver for prediction of prokaryote promoter elements and regulons. BMC Genomics 13:299. https://doi.org/10.1186/1471-2164-13-299.
31. Leong YK, Show PL, Ooi CW, Ling TC, Lan JC. 2014. Current trends in polyhydroxyalkanoates (PHAs) biosynthesis: insights from the recombinant *Escherichia coli*. J Biotechnol 180:52–65. https://doi.org/10.1016/j.jbiotec.2014.03.020.
32. Freches A, Lemos PC. 2017. Microbial selection strategies for polyhydroxyalkanoates production from crude glycerol: effect of OLR and cycle length. N Biotechnol 39(Part A):22–28. https://doi.org/10.1016/j.nbt.2017.05.011.
33. Wu H, Fan Z, Jiang X, Chen J, Chen GQ. 2016. Enhanced production of polyhydroxybutyrate by multiple dividing *E. coli*. Microb Cell Fact 15:128. https://doi.org/10.1186/s12934-016-0415-9.
34. Thanbichler M, Iniesta AA, Shapiro L. 2007. A comprehensive set of plasmids for vanillate- and xylose-inducible gene expression in *Caulobacter crescentus*. Nucleic Acids Res 35:e137. https://doi.org/10.1093/nar/gkm818.
35. Tsuge T, Taguchi K, Seiichi T, Doi Y. 2003. Molecular characterization and properties of *(R)*-specific enoyl-CoA hydratases from *Pseudomonas aeruginosa*: metabolic tools for synthesis of polyhydroxyalkanoates via fatty acid beta-oxidation. Int J Biol Macromol 31:195–205. https://doi.org/10.1016/S0141-8130(02)00082-X.
36. Liu W, Chen GQ. 2007. Production and characterization of medium-chain-length polyhydroxyalkanoate with high 3-hydroxytetradecanoate monomer content by *fadB* and *fadA* knockout mutant of *Pseudomonas putida* KT2442. Appl Microbiol Biotechnol 76:1153–1159. https://doi.org/10.1007/s00253-007-1092-8.
37. Kumar M, Singhal A, Verma PK, Thakur IS. 2017. Production and characterization of polyhydroxyalkanoate from lignin derivatives by *Pandoraea* sp. ISTKB 2:9156–9163.
38. Shi Y, Yan X, Li Q, Wang X, Liu M, Xie S, Chai L, Yuan J. 2017. Directed bioconversion of Kraft lignin to polyhydroxyalkanoate by *Cupriavidus basilensis* B-8 without any pretreatment. Process Biochem 52:238–242. https://doi.org/10.1016/j.procbio.2016.10.004.
39. Bauchop T, Elsden SR. 1960. The growth of micro-organisms in relation to their energy supply. J Gen Microbiol 23:457–469.
40. Lin L, Song H, Tu Q, Qin Y, Zhou A, Liu W, He Z, Zhou J, Xu J. 2011. The *Thermoanaerobacter* glycobiome reveals mechanisms of pentose and hexose co-utilization in bacteria. PLoS Genet 7:e1002318. https://doi.org/10.1371/journal.pgen.1002318.
41. Mercer AA, Loutit JS. 1979. Transformation and transfection of *Pseudomonas aeruginosa*: effects of metal ions. J Bacteriol 140:37–42.